



Comparison of artificial intelligence image processing with manual leucocyte differential to score immune cell infiltration in a mouse infection model of cystic fibrosis

Madeline G. Williams, Zachary J. Faber, Thomas J. Kelley *

Department of Genetics and Genome Sciences, Case Western Reserve University, Cleveland, OH, USA

ARTICLE INFO

Keywords:

Cystic fibrosis
Artificial intelligence
Leukocyte differential
Bronchoalveolar Lavage
Mouse model

ABSTRACT

Immune cell differentials are most commonly performed manually or with the use of automated cell sorting devices. However, manual review by research personnel can be both subjective and time consuming, and cell sorting approaches consume samples and demand additional reagents to perform the differential. We have created an artificial intelligence (AI) image processing pipeline using the Biodock.ai platform to classify immune cell types from Giemsa-stained cytopins of mouse bronchoalveolar lavage fluid. Through multiple rounds of training and refinement, we have created a tool that is as accurate as manual review of slide images while removing the subjectivity and making the process mostly hands off, saving researcher time for other tasks and improving core turnaround for experiments. This AI-based image processing is directly compatible with current workflows utilizing stained slides, in contrast to a change to a flow cytometry-based approach, which requires both specialized equipment, reagents, and expertise.

Introduction

Immune cell infiltration of the lung is a primary readout of infection severity in mouse models of cystic fibrosis (CF). *Pseudomonas aeruginosa* lung infection in CF mice results in having an exaggerated, neutrophil-dominated inflammatory response, mimicking the neutrophil response found in CF patients.^{1,2} Bronchoalveolar lavage fluid¹ is commonly collected and analyzed to determine the cytological nature of murine airways. Differential analysis of BALF involves the classification of stained immune cells into neutrophils, alveolar macrophages, and lymphocytes based on morphological features.

There is substantial variability in both the BALF collection and processing techniques.^{3–5} However, the recommendation for cytological analysis is preparing slides with a cytocentrifuge, staining with Wright-Giemsa, and using brightfield microscopy to count 300–500 cells.³ It has been found that larger sample sizes reflect the true cytological state of the lungs and cytocentrifugation helps the even distribution of cells. From that sample, the differentials are calculated into the percentage and total count for each cell type.

Manual review of Giemsa–Wright stained cytospin slides is laborious and time-consuming. Accurate identification of cell types based on morphological features suffers from differences in operator training and skill, cell staining, and cell distribution.^{3,5} This manual process is highly prone to

subjectivity, with large margins for intra- and inter-operator variability leading to a decrease in overall reproducibility.

To reduce these errors, the automation of cell differentiation for BALF is increasingly used in research laboratories. Whereas automated differentials are routine from blood samples, the reduced cellularity of other fluids, such as BALF, can lead to inaccurate results. New machines with BALF analysis capabilities are expensive, may require extensive operator training or expertise, and need additional adjustments to report reliable values.^{6,7}

BALF analysis using AI technology presents an exciting step forward from manual differentials. Deep learning networks are successfully being used to analyze BALF and other biological fluids, reducing the time and training required for accurate results.^{6–10} Knowledge of programming and costs bar these tools from being used on a larger scale. Biodock's platform facilitates the use of AI by offering easy to use labeling and image analysis tools.¹¹ Through these, we have expedited our BALF analysis process and minimize the subjective error of the manual counting in a way that retains accuracy and precision.

Results

We collected mouse BALF samples for cytological analysis. For each sample, a cytospin was prepared and Wright–Giemsa stained, then viewed and imaged under brightfield microscopy. Images for analysis were

* Corresponding author at: Department of Genetics and Genome Sciences, Case Western Reserve University, 825 BRB, 10900 Euclid Ave, Cleveland, OH 44106-4948, USA.
E-mail addresses: mwx912@case.edu (M.G. Williams), zxf102@case.edu (Z.J. Faber), tjk12@case.edu (T.J. Kelley).

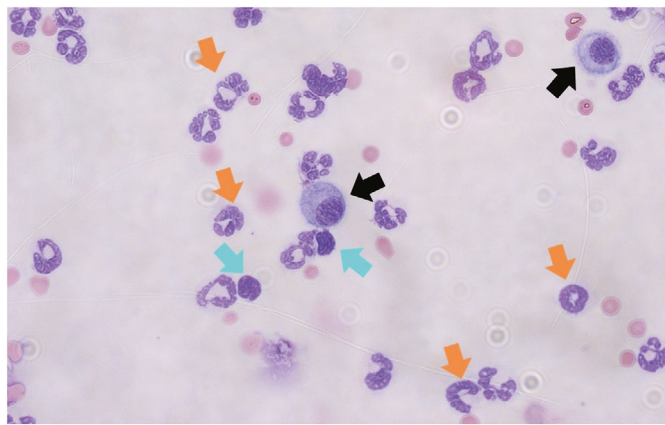


Fig. 1. Identified examples of Wright–Giemsa-stained neutrophils (orange arrows), macrophages (black arrows), and lymphocytes (blue arrows) at 400 times magnification. Mean area (pixels) for neutrophils is 1443.4, macrophage is 3851.0, and lymphocytes is 1435.2. (For interpretation of the references to colour in this figure legend, the reader is referred to the web version of this article.)

selected for even distribution of cells with distinct morphological features and clear examples of the desired cell classes for a three-part white blood cell differential: neutrophils, macrophages, and lymphocytes as shown in Fig. 1. Two different sets of images will be discussed, the training set and the test set. The training set is 189 digital images that were collected from 27 mouse BALF samples. These images were uploaded into Biodock and used to create and train the AI image analysis model. This model has five different versions, with the fifth iteration being the one selected for comparison. The test set of images were collected from 20 unique mouse BALF samples and consists of 86 images. The test set was both manually counted and then separately run through a Biodock analysis for cell counting. There is no overlap between the training images and the test images, to maintain the integrity of the test set.

The test set of 86 images were counted manually to establish a baseline for comparison. The cells were classified based on the presence of distinct morphological traits and comparison to expert-identified examples. There were two researchers who manually counted slides. There are lab-based scientists with basic cytology experience, but no formal pathology skills. Both researchers have no prior experience with AI technologies. This counting was all performed on the same day, averaging 2.56 min per slide. The manual counting portion of the analysis averages out to around 221 min for 86 slides. The actual time spent counting is closer to 265.2 min, likely from variabilities in cell number per slide. The totals for each cell type were calculated and grouped by mouse. Then taken as a percentage for each class out of the total number of cells per mouse. We take the percentages by mouse, aiming for a sample of around 200–300 cells counted per mouse. This data will function as our baseline for the test set, because manual counting is the golden standard for leukocyte differentials.³

The training set for the AI counting through Biodock’s image analysis software consisted of 189 digital images. Those 189 images were broken up into 1126 tiles for training based on a 1000 pixel average object size, based on the average size of neutrophils reported by Biodock and shown in Table 1 (S. Table 1). The tile and object size are used by the software

to optimize the object labeling. The model was trained in an iterative process with the definitive version of the model was built from the 189 images, with 18,259 neutrophil labels, 3317 macrophage labels, and 1133 lymphocytes (S. Table 2). These labels included examples of each cell type that had been positively identified by well-defined and visible features. The changes made in between versions include increased sample size, increased sample quality, removal artifacts, correction of mislabeled cells, and overall refining of the model output. These errors and other areas where the image analysis program struggled are shown in Fig. 2. Additionally, we determined that labeling additional cells present (erythrocytes, epithelial cells) did not help the distinguishing power of the model. These adjustments were made after assessing the output dashboard from the Biodock analyses, from which we manually identified problems with the AI labels. The end result was a model version that best correlated with the manual counts and had removed as many artifacts as possible.

To test the AI model, the test set was then uploaded to Biodock. The 86 digital images were uploaded to the Biodock file system as JPEGs and analyzed using the finalized model version. The analysis took 3 min and 59 s to complete. All images were analyzed simultaneously. Analysis data were organized into Biodock’s data dashboard and exported into a Microsoft Excel workbook. The primary output of the analysis we utilized was the number of objects counted (labels created) for each class. We collected these data by mouse and calculated the percentage of each class per mouse to match the calculations performed on the manual data.

The analysis from Biodock also contained characteristic data for every label created by the AI. For every objected labeled, Biodock reported the image ID, cell class(predetermined by the labeling step), area (number of pixels the label covers), eccentricity (measure of how elliptical an object is), perimeter (count of pixels over the outer boundary of the object), solidity (A measurement of the overall concavity of an object), X position, Y position, average intensity (based on different color channels), and model score. These characteristics allowed us to better understand how the AI was seeing the different classes and to easily visualize the patterns and relationships within the dataset. We used primarily area and solidity to determine outliers and find artifacts produced by the AI. Fig. 3 shows the scatter plot between these two variables provided by the data dashboard on Biodock. The further from one on the solidity axis was determined to be irregularly shaped labels. Fig. 3B shows a sample of the smallest objects identified for the test set. Further investigation into those labels revealed that they were often mislabeled artifacts. We know the average size of labels in each class. Whereas the size differs between macrophages and lymphocytes and neutrophils, the average for size stays consistently above a certain threshold. Knowing the size allows us to determine a threshold for what sized label could no longer truly be considered a cell, 500 pixels. We filtered the object labels for all three classes by this area threshold, recounted the labels, and recalculated the percentages for each class. The “filtered” dataset is filtered by 500 and the “raw” dataset is unmodified output of the AI analysis. The filtering allowed us to objectively remove artifacts created by the AI analysis process consistently across all of the images.

To compare the AI method to the manual method, we used the calculated class percentages from the manual and AI analyses. The percentages are the desired output for our infection models and are standard for manual differentiation of leukocytes.^{1,2} They also best serve to compare slides that do not have the same number of cells, as that number varies from mouse to mouse. In the AI analysis, the actual cell number counted in the AI model is inflated compared to the manual counts, likely due to artifacts produced by the AI: labeling mucus, dye, mislabeling cells, or labeling partially visible cells. Filtering helps significantly reduce this inconsistency. Our approach for comparison begins with assessing the distribution for the test set for each method in a box plot in Fig. 4 along with calculating mean and standard deviation in Table 2. We can visually compare the results of the counting methods and see the outliers or any obvious trends with the data using the box plot. The relationship between the manual and AI methods was plotted in a Bland–Altman plot for each class in Fig. 5. The Bland–Altman plot uses the differences in percentages for each class to display bias (reported as the mean difference) and trends within the data. The

Table 1
Mean label area by pixel for each class of cells differentiated. These are the label averages reported by Biodock from the 5th version of the model.

Label class	Mean area (pixels)
Neutrophil	1443.4
Macrophage	3851.0
Lymphocyte	1435.2

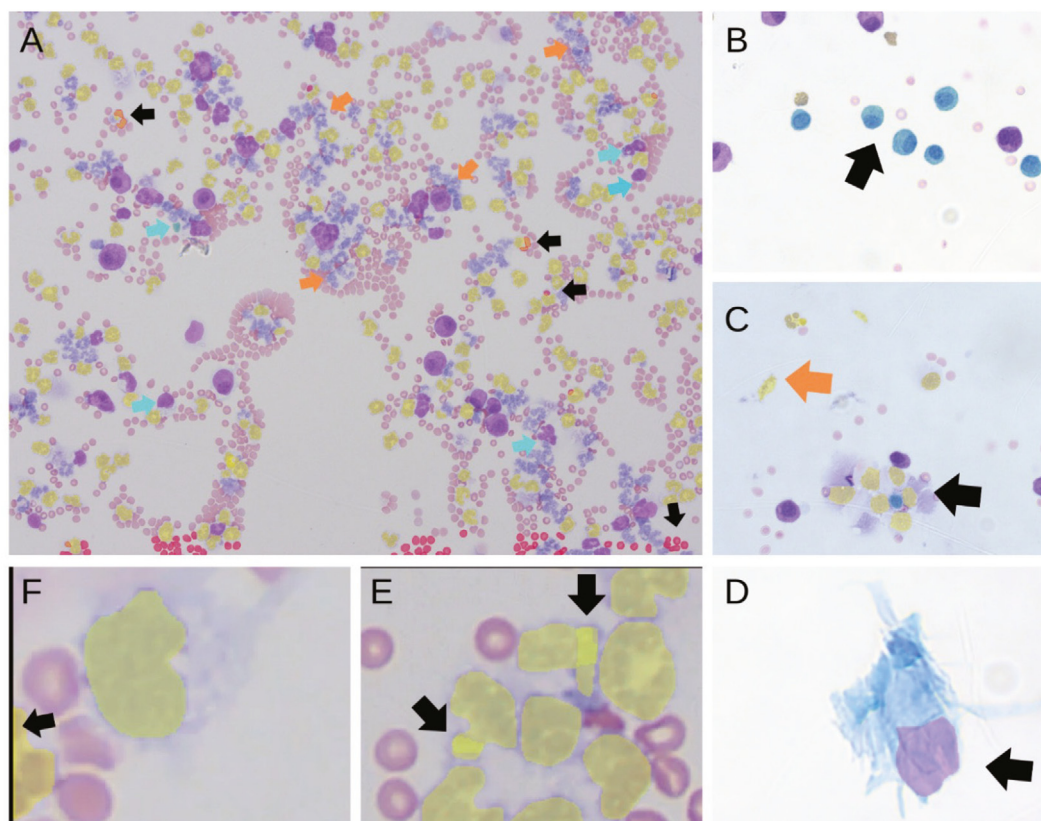


Fig. 2. Digital slide images with annotations from Biodock analysis output, with the errors found commonly in earlier versions of the model that prompted fixing. (A) Densely populated images not being fully labeled in earlier version, with mislabeled cells (teal), RBCs inconsistently labeled and overlapping existing labels (black arrows), cells not being labeled (orange arrows). (B) Incorrect labeling of cell type. (C) Epithelial cells being mislabeled as neutrophils, lymphocytes, or macrophages due to morphological similarities (black arrows), dyed artifacts being mislabeled as neutrophils (orange arrows). (D) Labels being created on stained artifacts on the slides inconsistently dyed RBCs labeled as lymphocytes or neutrophils. (E–F) Rectangular artifacts that overlap correct labels, created on the sides or edges of stained cells. (For interpretation of the references to colour in this figure legend, the reader is referred to the web version of this article.)

bias reported between the manual percentage and the AI percentage for neutrophils in Fig. 5A is -0.2 and the upper limits of agreement were -7.44% to 7.04% . Fig. 5B shows macrophages and the bias there is -0.3 (-6.201 – 5.601%) and in Fig. 5C it is 0.5500 (-3.832 to 4.932%) for lymphocytes. The Spearman correlation coefficient assess correlation of different methodology for non-normal data and is shown for the final, filtered version of the test set in Fig. 6 and for all versions in Sup. Fig. 1. The Spearman correlation coefficient between the two methods for all three class populations: $r = 0.9846$ for neutrophils, $r = 0.9743$ for macrophages, and $r = 0.8250$ for lymphocytes. Performing the two-sample t -test with equivalent variance allows us to test if the manual percentages are significantly different from the AI differentiated percentages. The t -stat for neutrophils is -0.0353 , for macrophages is 0.0342 , and for lymphocytes is 0.0363 , all with 38 degrees of freedom. This suggests a very low difference in the sample means from each method in all three classes. The P two-tail value is 0.972 for neutrophils, 0.9629 for macrophages, and 0.9319 for lymphocytes at ($\alpha = 0.05$). This means that at either end of the distribution, there is no significant difference between the values from each method.

Discussion

This study evaluates and compares the manual and automated process of differentiating leukocytes in BALF. Our model, which was developed to identify murine leukocytes, demonstrates its capabilities successfully with our test set. It accurately replicates the manual differentiating power of a trained professional in a fraction of the time and removes the possibility of human error. Whereas there are commercial solutions for blood for

humans and animals,^{4,6} the BAL samples collected from mice were not detected in hematological machines available to us. This finding is significant as most human BAL studies are still quantified by flow cytometry or manual counting.² Identifying an automated, quantitative method that does not destroy the patient sample would be a valuable addition to human clinical studies. This goal led us to try Biodock as an affordable and easily accessible option to experiment with while continuing to manually count cytological slides. Additionally, Biodock's system allows the model to be fully customized to the needs of the researcher. The limits for analysis only exist within the expertise and time available for labeling cells and tissues. The Biodock AI model has allowed us to automate our BALF processing without the need for expensive equipment or extensive training. It also allows us the flexibility to manually review and adjust the automated process, as well as allowing us to customize a model for our specific laboratory needs. The use of an AI model seamlessly fits our existing workflow and does not destroy or require more sample BALF for processing.

This pipeline for differential counts greatly reduces the analysis time, allowing quick turnover over and faster report times on experiments. The process of labeling and training the model for analysis still is time-consuming, but essential for the AI to best reflect the researcher's expertise in the various model iterations. Biodock training program expedites this process by offering AI object segmentation tools powered by a variation of the Segment Anything Model, a deep learning model whose usefulness is recognized in medical imaging analysis.¹² With an average analysis time of 2.65 min per slide image, training the AI using the training set of 186 images would take around 8 h to label and 1 h to spin up the model. It can be trained and adjusted faster using the tools, leading to more extensive models with a larger range of examples and number of object examples.

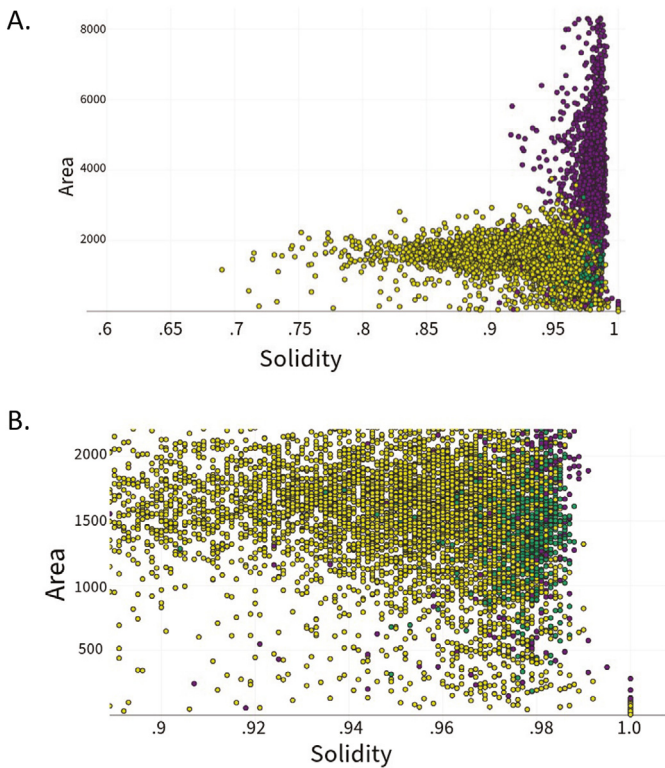


Fig. 3. Area vs Solidity scattergram from Biodock's Data Dashboard. Yellow is neutrophils, purple is macrophages, and green is lymphocytes. (A) The distribution of all the test set cells from version 5 of the model. (B) A zoomed in view of the scattergram with area between 2500 pixel and solidity scored between 0.9 and 1.0. The irregularity of the data in this area, especially below 1000 pixels suggests a high number of artifacts in the data. At 0 area and 1 solidity score, those are also artifacts, which often overlap with accurate labels and are found at the edges of slides. (For interpretation of the references to colour in this figure legend, the reader is referred to the web version of this article.)

The iterative model creation process, once completed, can be used on an unlimited number of slide images for analysis. A Biodock analysis takes only 4 min for the file size that we use. The time saved from using the pipeline has well made up for the time spent training.

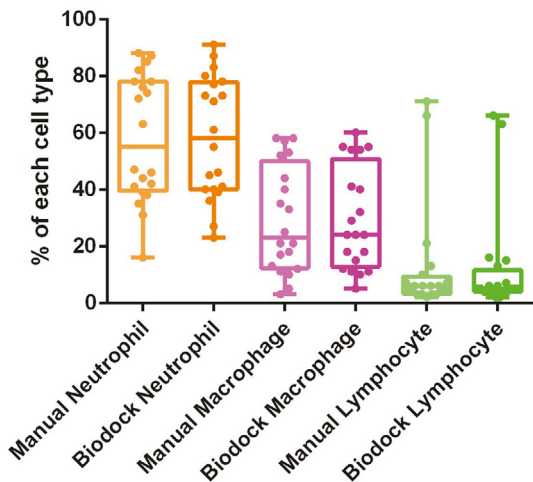


Fig. 4. Manual vs AI comparison of the test set data. This box plot shows the distribution of the percentages side by side for comparison of the two methods. Additionally, it shows each data point represented as a point within the distribution, demonstrating reproducibility of the data.

Table 2

The mean and standard deviation for the test set for comparison between manual and AI methodologies. The mean is slightly higher in the AI method for neutrophils and macrophages, but slightly lower than the manual method for lymphocytes. This difference is statistically insignificant, with the *P* two-tail value being 0.972 for neutrophils, 0.9629 for macrophages, and 0.9319 for lymphocytes at ($\alpha = 0.05$) for the two-sample *t*-test assuming equal variance. These values being higher than 0.05 means that there is not a significant difference between the mean output from the two different methods for all three classes.

	Mean	Standard deviation
<i>Manual</i>		
Neutrophil	0.581	0.050
Macrophage	0.294	0.042
Lymphocyte	0.125	0.044
<i>Biodock (AI)</i>		
Neutrophil	0.583	0.048
Macrophage	0.296	0.040
Lymphocyte	0.120	0.041

1. Balfour-Lynn IM, Laverty A, Dinwiddie R. Reduced upper airway nitric oxide in cystic fibrosis. *Archives of disease in childhood*. Oct 1996;75(4):319–22.
2. Davidson KR, Ha DM, Schwarz MI, Chan ED. Bronchoalveolar lavage as a diagnostic procedure: a review of known cellular and molecular findings in various lung diseases. *J Thorac Dis*. Sep 2020;12(9):4991–5019. [10.21037/jtd-20-651](https://doi.org/10.21037/jtd-20-651).
3. Al-Shargie F, Tareh SM, Al-Ezzi A. Mental Stress and Cognitive Deficits Management. *Brain Sci*. Mar 27 2024;14(4)<https://doi.org/10.3390/brainsci14040316>.

Furthermore, by automatically applying the learned expertise of a researcher, the AI pipeline improves the objectivity of the analysis. Manual analysis of cytology slides is not only a time-consuming task, but also a repetitive one that relies on consistent application of expertise for an extended period of time. It is acknowledged that tasks such as these suffer from vigilance decrement, with a decline in observer performance as the time on task lengthens.³ The Biodock model helps eliminate this factor in our inflammatory analysis.

In comparing the AI model to the manual methods, we were able to get consistent percentages for all three classifications of leukocytes. Comparing the mean and standard deviation values between the manual and AI methods showed that both methods have remarkably similar distributions. In the Bland–Altman difference plot, where the mean difference (bias) between the two methods is plotted against the average, the bias for all three classes is close to zero: -0.2 for neutrophils, -0.3 for macrophages, and 0.55 for lymphocytes. The slight negative bias for neutrophils and macrophages suggests that the AI model overcounts those values, but undercounts lymphocytes. Additionally, many of the differences on the Bland–Altman plot are within the 95% limits of agreement, which suggest that the methods are comparable. This is further supported through the Spearman correlation coefficients ($r = 0.9846$ for neutrophils, $r = 0.9743$ for macrophages, and $r = 0.8250$ for lymphocytes) which confirms that there is a strong association between the manual and AI data.

Major differences between some of the manual and automated counts stem from irregular samples. We have noted that both extremely high and low cell counts lead to abnormal results. Images that are outliers can be flagged for manual review. Manual review of an automated analysis allows for full access to every object mask made and adjustments to cells that were mislabeled or unlabeled can be made directly in Biodock. This updates the overall data without changing the slides. Whereas debris is regularly seen on our inflammatory slides, the model's overall accuracy with cell identification is still overall consistent with manual review. It is reported that increasing the number of cells examined does increase the accuracy of automated cell differentials.⁶ By using percentages, we were able to standardize the data for better comparison, but there is a need to further refine the model to report cell counts with better resolution.

This tool does not limit itself to just the expedited differential process and the labeling of three types of leukocytes cells. Our acute infection model analyses weight, inflammation levels, and CFU recovery holistically to assess mouse recovery. By using percentages from the differential analysis, we get an idea of their inflammation profile and keep the neutrophil

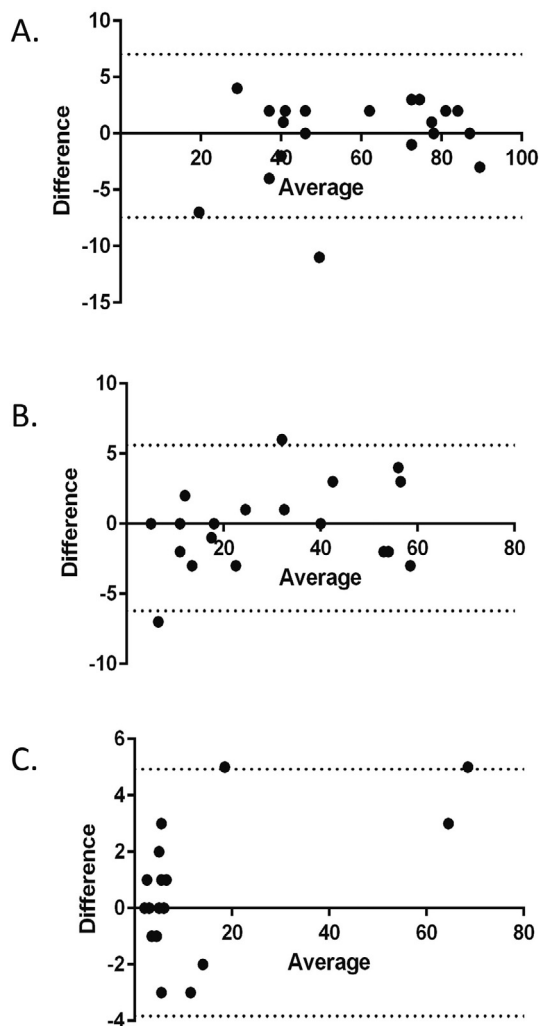


Fig. 5. Agreement between artificial intelligence and manual differentiated counts of neutrophils (A), macrophages (B), and Lymphocytes (C) displayed in Bland–Altman difference plots. These graphs show the agreement between the two methods and demonstrate any bias. (Mean difference should have a line that the points are using) The dotted lines represent the 95 % confidence interval for the mean difference. For neutrophils, the mean difference was -0.2% , the lower limit is -7.44% , and the upper limit of agreement is 7.04% .

percentage in mind primarily as a level of their response. The AI was primarily trained to perform this differential analysis exactly as we would have done it manually. However, within Biodock's system, there is a host of information that has yet to be utilized within the scope of this

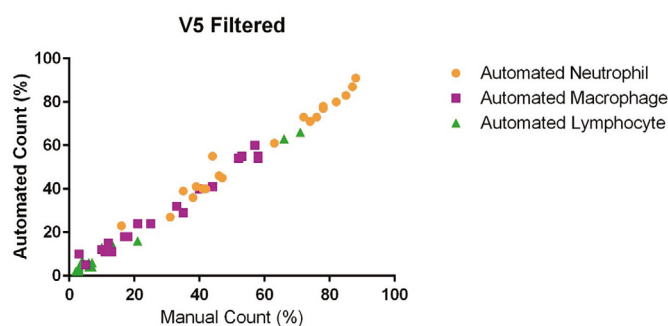


Fig. 6. The agreement between the manual differentiated and AI (artificial intelligence) differentiated cell counts. The V5 filtered version is the final version used for analysis.

comparison. For every analysis run, you have full visualization of every slide, and every object mask created along with access to size, eccentricity, and intensity data for each of them. Biodock allows you to visualize that data in different ways within the context of the experiment. There is a great deal of potential within that data to expand the use of the slides beyond the differential analysis. We used size to filter artifacts, based on the average size of all the cells. However, cell area, which is reported for every object labeled, could be utilized in other ways. In alveolar macrophages found in BALF, cell size has been reported to be related to clearance abilities.¹³ Already collected data from the differential analysis could be used for a number of different applications, expanding the value of having a dedicated AI for a project.

The entire project, from training the model to the analysis of the slides, was done with no prior knowledge of AI technology for any research-related purposes. It was also done with little to no coding experience needed. Although Biodock is definitely a more powerful tool with coding and computer skills, it was not needed to create an accurate and effective model for our research purposes. There was no cost involved in any of the pipeline creation process outside of the time it took to put it together. This factor, paired with its potential expanded value and accuracy when compared to manual analysis, makes this pipeline an affordable and incredibly accessible way for someone to use AI for biological research. It is a quick and straightforward way to get the information without investing in expensive machinery, training, or programs. It is a great starting point to optimize image processing for any researcher's project.

Conclusion

This study demonstrates the capabilities of an AI model created through the website Biodock that was trained by a researcher without programming to differentiate leukocytes in murine BALF. The model can accurately produce the percentages that correlate well and have no bias or significant difference with manually differentiated percentages performed by trained professionals in a fraction of the time and without human bias. This automation of this process using AI greatly expedites the data collection and processing of our mouse experiments and enables us to tackle larger tasks in the way of CF mouse research.

Methods

Sample collection and processing

Bronchoalveolar lavage fluid samples in this study were collected from mouse infection experiments following the recommended procedure.^{1,3} 100 ml of BALF was added to one chamber of a Fisherbrand Double Cytology funnel, which was clamped to an Eprelia coated Double Cytoslide. Cells were spun at 750 ml for 5 min. Cytoslides were fixed with cold methanol and were Wright–Giemsa stained. Prepared slides were then viewed with the Axio Observer. Z1 / 7 microscope under the Plan-Apochromat 20 \times /0.8 M27 objective. 3–10 digital images were taken of each sample using the Axio 105 Color Right, capturing a monolayer of stained cells with even distribution. The objective was to capture between 100 and 300 cells between the images, following the sample size recommendation.

Manual classification and counting

All digital images included in the test set were manually differentiated to act as a baseline for comparison to the AI calculations. We counted digital images of stained slides, classifying the different cell types based on morphological features. The total number of neutrophils, macrophages, and lymphocytes per image was recorded. There were epithelial cells and RBCs visible on the slide, however, they were not part of the differential and therefore not counted. These numbers were grouped for the total number of each class per mouse (one slide per mouse). The percent of each cell type was calculated.

AI labeling using Biodock

To create an automated workflow to score BAL immune differentials, we utilized Biodock.ai, a web-based deep AI platform for image analysis. Our training images were uploaded as JPEGs into a Biodock project for labeling. Labeling consists of manually differentiating and organizing the cells in the image into different “object classes”. These labels are created using Biodock's different AI tools, which uses SAM technology to better draw shapes around the cells. The object classes for neutrophil, macrophage, and lymphocyte were sized at 1000 pixels, therefore Biodock's training platform divides the image into 6 smaller sections for better recognition of labels. The labeled objects were then used to train an AI image analysis model that utilizes an Alligator architecture. The model is broken up into versions, with each version being the output of the set of training labels. After the initial version, Biodock grants access to an additional labeling tool, “AI Pre-Label”, which uses the classification capabilities of the existing model to further train the next version. This feature assigns near-instant labels to the slide images which then need to be manually curated by the individual training the model. The idea of this tool is to increase the total number of objects labeled and the number of images included in the next model version. After a model has been trained, it can be used in an analysis, with Biodock's official recommendation being to not use the first version of a model for analysis. A Biodock analysis uses the model at a given version to automatically label the digital slide images. The data made available are organized per group, as well as each individual object.

AI classification and counting using Biodock

These are cytospin slides that were digitally imaged, however, those images were not used in any of the training of the AI model. We grouped the 86 digital images into folders by mouse # and they were uploaded to a Biodock analysis. The analysis uses the trained AI model to automatically label digital images of stained slides. Biodock's labels for each class are assigned independently and simultaneously, therefore one class's labeled objects do not affect another. We then used the data from this analysis at the individual object level, where Biodock recorded metrics like area, perimeter, and solidity for every individual object recorded. From here, we calculated the percentage of each cell type from the total number of cells labeled, per mouse. Additionally, we ran the same test set through analysis using the earlier versions of the AI model. From each of these analyses, we grouped the data by mouse and calculated the percentages of each class.

Comparison of manual differentiation to AI differentiation of WBC

We compared the manual and AI methodology through analysis of the test set data. We calculated the percentages for each class for the manual counts and percentages for the object counts from the Biodock analysis. We calculated the mean, standard deviation, and plotted the distribution of the test set in a box plot. Agreement between the two methods was

assessed through the Bland–Altman difference plot and the Spearman correlation coefficient calculation. We performed a two-sample *t*-test, assuming equal variances, to assess equivalence of the two methods.

Acknowledgements and Funding

This work was supported by CF Mouse Core Grant CFFHODGES23R1.

Declaration of competing interest

All authors declare that none have any conflicts of interest associated with this work.

Appendix A. Supplementary data

Supplementary data to this article can be found online at <https://doi.org/10.1016/j.jpi.2025.100438>.

References

- Rosenjack J, Hodges CA, Darrah RJ, Kelley TJ. HDAC6 depletion improves cystic fibrosis mouse airway responses to bacterial challenge. *Sci Rep* 2019; 910282. <https://doi.org/10.1038/s41598-019-46555-4>.
- van Heeckeren AM, Schluchter MD, Xue W, Davis PB. Response to acute lung infection with mucoid *Pseudomonas aeruginosa* in cystic fibrosis mice. *Am J Respir Crit Care Med* 2006;173(3):288–296. <https://doi.org/10.1164/rccm.200506-917OC>.
- Baughman RP. Technical aspects of bronchoalveolar lavage: recommendations for a standard procedure. *Semin Respir Crit Care Med* 2007;28(05):475–485. <https://doi.org/10.1055/s-2007-991520>.
- Kalidhindi RSR, Ambhore NS, Sathish V. Cellular and biochemical analysis of bronchoalveolar lavage fluid from murine lungs. *Methods Mol Biol* 2021;2223:201–215. https://doi.org/10.1007/978-1-0716-1001-5_15.
- Jacobs JA, De Brauwier E. BAL fluid cytology in the assessment of infectious lung disease. *Hosp Med Aug* 1999;60(8):550–555. <https://doi.org/10.12968/hosp.1999.60.8.1172>.
- Lapsina S, Riond B, Hofmann-Lehmann R, Stirn M. Comparison of Sysmex XN-V body fluid mode and deep-learning-based quantification with manual techniques for total nucleated cell count and differential count for equine bronchoalveolar lavage samples. *BMC Vet Res Feb* 5, 2024;20(1):48. <https://doi.org/10.1186/s12917-024-03884-5>.
- Tao Y, Cai Y, Fu H, Song L, Xie L, Wang K. Automated interpretation and analysis of bronchoalveolar lavage fluid. *Int J Med Inform Jan* 2022;157, 104638. <https://doi.org/10.1016/j.ijmedinf.2021.104638>.
- Sadeghi H, Braun HS, Panti B, Opsomer G, Bogado Pascottini O. Validation of a deep learning-based image analysis system to diagnose subclinical endometritis in dairy cows. *PLoS One* 2022;17(1), e0263409. <https://doi.org/10.1371/journal.pone.0263409>.
- Smith KP, Kang AD, Kirby JE. Automated interpretation of blood culture gram stains by use of a deep convolutional neural network. *J Clin Microbiol Mar* 2018;56(3). <https://doi.org/10.1128/jcm.01521-17>.
- Marzahl C, Aubreville M, Bertram CA, et al. Deep learning-based quantification of pulmonary hemosiderophages in cytology slides. *Sci Rep Aug* 3, 2020;10(1):9795. <https://doi.org/10.1038/s41598-020-65958-2>.
- Biodock. Biodock, AI Software Platform. www.biodock.ai.
- Sun Y, Zhang K, Qi H, Zhang H, Zhang S, Bi Y, Wu L, Sun L, Qi J, Liu D, Ma J, Tein P, Lie W, Li J. Computational predicting the human infectivity of H7N9 influenza viruses isolated from avian hosts. *Transbound Emerg Dis* 2021;68:846–856.
- Krombach F, Münzing S, Allmeling A-M, Gerlach JT, Behr J, Dörger M. Cell size of alveolar macrophages: an interspecies comparison. *Environ Health Perspect* 1997;105(suppl 5):1261–1263.